Brief intraperitoneal radioimmunotherapy of small peritoneal carcinomatosis using high activities of noninternalizing 125I-labeled monoclonal antibodies.

Vincent Boudousq, Stéphanie Ricaud, Véronique Garambois, Caroline Bascoul-Mollevi, Samir Boutaleb, Muriel Busson, François Quenet, Pierre-Emmanuel Colombo, Manuel Bardiès, Pierre-Olivier Kotzki, et al.

Brief intraperitoneal radioimmunotherapy of small peritoneal carcinomatosis using high activities of non-internalizing ^{125}I-labeled monoclonal antibodies

Vincent Boudousq[1,4], Stéphanie Ricaud[1], Véronique Garambois[1], Caroline Bascoul-Mollevi[2], Samir Boutaleb[1], Muriel Busson[1], François Quenet[2], Pierre-Emmanuel Colombo[2], Manuel Bardiès[3], Pierre-Olivier Kotzki[1,4], Isabelle Navarro-Teulon[1], André Pèlegrin[1] and Jean-Pierre Pouget[1,5]

[1] IRCM, Institut de Recherche en Cancérologie de Montpellier, Montpellier, F-34298, France; INSERM, U896, Montpellier, F-34298, France; Université Montpellier1, Montpellier, F-34298, France; CRLC Val d'Aurelle Paul Lamarque, Montpellier, F-34298, France; [2] CRLC Val d'Aurelle-Paul Lamarque, F-34298 Montpellier, France; [3]INSERM, U892, F-44000 Nantes, France; [4] Service de Médecine Nucléaire, CHU de Nîmes, Nîmes F-30029, France; [5] Direction de la Radioprotection de l'Homme, Institut de Radioprotection et de Sûreté Nucléaire, Fontenay-aux-Roses, F-92262 France;

To whom correspondence may be addressed: Jean-Pierre Pouget, Institut de Recherche en Cancérologie de Montpellier, CRLC Val d'Aurelle, 34298 Montpellier Cedex 5, France.

E-mail: jean-pierre.pouget@valdorel.fnclcc.fr

Contact information 1st author: Vincent Boudousq, Institut de Recherche en Cancérologie de Montpellier, CRLC Val d'Aurelle, 34298 Montpellier Cedex 5, France.

E-mail: vincent.boudousq@chu-nimes.fr

Words count of the manuscript: 5998 words

This work was supported by the Institut National du Cancer, grant R09080FF / RPT09005FFA.

Running title: Brief intraperitoneal ^{125}I-mAbs RIT

Abstract

We assessed the efficiency and toxicity of brief-intraperitoneal radioimmunotherapy (Bip-RIT) using high activities of ^{125}I-labeled monoclonal antibodies (mAbs) in the treatment of small volume peritoneal carcinomatosis. **Methods:** For Bip-RIT, athymic nude mice with peritoneal tumor xenografts were i.p. injected at day 4 post-graft with 185 MBq of ^{125}I-35A7 (anti-CEA mAb) (740 MBq/mg) and, after one hour, the peritoneal cavity was abundantly washed with saline solution to remove unbound radioactivity (Bip-^{125}I-35A7-RIT). Another group of mice received Bip-RIT and one intravenous (iv) injection of 37 MBq of ^{125}I-35A7 at day 7 or 11 after graft (Bip+ivd7- or Bip+ivd11-^{125}I-35A7-RIT). Control groups were treated with saline solution (Bip-NaCl) or with the irrelevant PX mAb (Bip+ivd7-^{125}I-PX-RIT). Tumor growth was followed by bioluminescence and SPECT-CT imaging and hematological toxicity evaluated by complete blood count. Survival time was reported and mice were sacrificed when the bioluminescence signal reached 4.5×10^7 photons/s. The biodistribution of ^{125}I-35A7 mAbs after iv- or Bip-RIT was assessed and the mean absorbed irradiation dose by organs and tumors was calculated using the MIRD formalism. **Results:** Mild, transient hematological toxicity was observed after Bip+iv-^{125}I-mAbs-RIT while no weight loss was reported. Median survival was increased from 32 d for the control groups to 46 d in the Bip-^{125}I-35A7-RIT group, to 66 d in Bip+ivd11-^{125}I-35A7-RIT mice and to 73 d in the Bip+ivd7-^{125}I-35A7-RIT group. Bip-^{125}I-35A7-RIT resulted in 3-fold higher tumor-to-blood uptake ratio than iv-^{125}I-35A7-RIT and the mean absorbed irradiation doses by tumors were 11.6 Gy (Bip-RIT) and 16.7 Gy (iv-RIT). For healthy tissues other than blood, the mean absorbed irradiation dose did not exceed 1 Gy following Bip-RIT and 4.2 Gy after iv-RIT.

Conclusion: The efficiency, low toxicity and high tumor-to-healthy tissues uptake ratio associated with Bip-^{125}I-35A7-RIT suggest that this methodology could be used in

combination with radiation synergistic drugs in the therapy of small volume peritoneal carcinomatosis following cytoreductive surgery.

Keywords: radioimmunotherapy, Auger electrons, peritoneal carcinomatosis

INTRODUCTION

Peritoneal carcinomatosis is a common evolution of gastrointestinal or gynecological tumors, or of primary peritoneal malignancy like mesotheliomas or peritoneal serous carcinoma. Peritoneal carcinomatosis has been considered for long time as a terminal disease with a median survival ranging between 12 and 23 months for patients with stage IV ovarian cancer, about 6 months for colorectal carcinoma, 3 for gastric cancer, 2 for pancreatic cancer and only 1.5 months for carcinomatosis from unknown primary cancer (for reviews (*1*,*2*)). The therapeutic approach is based on palliative systemic chemotherapy and surgery is mainly used in palliative intention, according to symptoms, except in the case of ovarian cancer where complete cytoreduction is part of the standard therapeutic regimen. Twenty years ago, Sugarbaker introduced cytoreductive surgery (CRS) to resect the visible disease combined with hyperthermic intraperitoneal chemotherapy (HIPEC) to treat the residual disease, as an innovative therapeutic option for selected patients with peritoneal carcinomatosis (*3*,*4*). CRS procedure depends on the extent of the peritoneal disease and the chemotherapy protocols may include mitomycin C, oxaliplatin, mitoxantrone, cisplatin and irinotecan alone or in combination (for reviews (*1*,*2*)). HIPEC can be performed using open or closed abdomen techniques and perfusion may vary from 30 min to 90 min. Although the consensus about the ideal technique is not clear, CRS-HIPEC has been shown to improve survival of patients with peritoneal dissemination from peritoneal pseudomyxoma, colorectal cancer, and diffuse peritoneal mesothelioma ((*5*,*6*) and for reviews (*1*,*2*)). Although mortality is relatively low, morbidity results from surgery complications and/or from toxicity (such as leucopenia, anemia, thrombopenia, heart, liver or renal toxicity) due to the cytostatic agents (for reviews (*1*,*2*)).

Several studies in rodents have shown that radioimmunotherapy (RIT) could be used efficiently as an adjuvant treatment after CRS for the treatment of peritoneal carcinomatosis

(*7-9*). Several intraperitoneal (i.p.) RIT studies using strong energy beta or alpha emitters are ongoing in animals (*8-13*). So far, five antibodies (against MUC1, CA-125, TAG-72 and gp38) have been conjugated to four β-emitting radionuclides for i.p. RIT in patients with ovarian cancer (for review (*14*)). Based on previous encouraging results (*15-19*), a phase III randomized multicenter study was undertaken (*20*) in which the efficiency of conventional chemotherapy was compared with i.p. injection of ^{90}Y-labeled HMGF1 murine mAb (anti-MUC1). However no improvement in survival was observed after RIT, although peritoneal recurrence was significantly delayed. One explanation was that the irradiation dose delivered to the tumors was not high enough and that i.p. injection alone did not target all tumor deposits. Indeed, the induced toxicity by beta- and gamma-emitters is a drawback for a treatment scheme using repeated injections. One alternative could be the use of short range particles like alpha emitters (*21*) or Auger electron emitters. We previously showed that anti-CEA mAbs labeled with Auger electron emitters and intravenously (i.v.) injected in mice xenografted with cancer cells could significantly delay the growth of small peritoneal solid tumors (*22*, *23*). We thus wanted to assess the efficiency and toxicity of ^{125}I-mAbs when used in i.p. RIT in mice bearing small peritoneal tumors. In addition, since to our knowledge the effects of i.p. RIT carried out following the HIPEC protocol have never been investigated, we decided to carry out RIT using closed peritoneal perfusion of ^{125}I-labeled anti-CEA mAbs for a short period (1 h), followed by extensive washing of the peritoneal cavity with saline solution to remove the unbound radioactivity. We named this procedure brief-intraperitoneal RIT (Bip-RIT).

MATERIALS AND METHODS

Cell line and monoclonal antibodies

The vulvar squamous carcinoma cell line A-431 expressing the Epidermal Growth Factor Receptor (EGFR or HER1) and transfected as previously described in (*22*), with constructs encoding the *CarcinoEmbryonic Antigen* (*CEA)* and *luciferase* genes was used. Cells were grown as described in (*22*). The non-internalizing murine IgG1k 35A7 mAb, specific for the CEA Gold 2 epitope, was used to target CEA. The irrelevant PX antibody was used for control experiments. PX is an IgG1 mAb that has been purified from the mouse myeloma MOPC 21 (*24*). PX and 35A7 were purified from mouse hybridoma ascite fluids by ammonium sulfate precipitation followed by ion exchange chromatography on DE52 cellulose (Whatman, Balston, United Kingdom).

Radiolabeling

Iodine 125 (^{125}I) was from Perkin Elmer (Boston, MA, USA) and mAbs were radiolabeled at the specific activity of 740 MBq/mg for RIT and biodistribution studies, using the IODO-GEN method and as described in (*22*). The immunoreactivity of ^{125}I-mAbs against CEA was assessed *in vitro* by direct binding assay (*22*). The binding percentage was determined by measuring the antigen-bound radioactivity after two washes with PBS and was between 50-60%.

Animals

Athymic nude mice (6-8 week/old females) were obtained from Charles River (Lyon, France) and were acclimated for 1 week before experimental use. They were housed at 22°C and 55% humidity with a light/dark cycle of 12h. Food and water were available *ad libitum.* The day before RIT, force-feeding with Lugol's solution was performed and stable iodine was added in drinking water for the entire experimental period. Body weight was determined weekly and clinical examinations were carried out throughout the study. Hematologic toxicity was

monitored during 70 d after the beginning of RIT, using the scil Vet abc system (SCIL Animal Care Company, Altorf, France). All the animal experiments were performed in compliance with the French guidelines and INSERM standards for experimental animal studies (Agreement no. B34-172-27).

RIT experiments

Mice were i.p. grafted with 0.7×10^6 A-431 cells suspended in 0.3 ml DMEM medium. Tumor growth was assessed 3 days after cell xenograft by bioluminescence imaging that allowed the segregation of mice in homogeneous groups. Four days following grafting, mice were treated by brief intraperitoneal radioimmunotherapy (Bip-RIT) or intraperitoneal RIT (ip-RIT).

The protocol used for Bip-RIT was as follows. Mice were anaesthetized by i.p. injection of a solution containing 100 mg/kg ketamine (Ketamine™ Panpharma; Panpharma, Fougère, France) and 1 mg/kg medetomidine (Dormitor™; Pfizer, Paris, France). Then, they were i.p. injected with either NaCl or ^{125}I-mAbs in a final volume of 5 mL. One hour later, the peritoneal cavity was flushed with 25 mL NaCl for 15 min, using a perfusion system adapted from Aarts *et al.* (*8*). Typically, an inflow needle was placed in the upper part of the abdominal cavity and two multiperforated catheters were inserted laterally through the abdominal wall to be used as outflows (Fig. 1A). Perfusion was done using a peristaltic pump (Harvard apparatus, Les Ulis, France). Once the wash of the peritoneal cavity was terminated, the catheters were removed and mice were weighted. Mice were then awakened by i.p. injection of atipamezole™ (Antisedan 2.5 mg/kg body weight, Pfizer, Paris, France).

Ip-RIT consisted of standard i.p. injections of saline solution (NaCl) or ^{125}I-mAbs (final volume of 5 mL) without wash of the peritoneal cavity and iv-RIT at day 7 or 11 was conventionally done as described in (*22*).

Specifically, for Bip-RIT, one group of mice (n=8) was treated with 5 mL of NaCl (Bip-NaCl) and another (n=10) with 185MBq ^{125}I-35A7 mAb (Bip-^{125}I-35A7-RIT). In the case of ip-RIT, the control group (n=7) received one i.p. injection of 5mL NaCl (ip-NaCl), while the other group of mice (n=15) received one i.p. injection of 37 MBq of ^{125}I-35A7 mAb at day 4 and one at day 7 post-graft (ip+ipd7-^{125}I-35A7-RIT). For the combined Bip+iv-RIT, mice received Bip-^{125}I-35A7-RIT at day 4 post-graft and one i.v. injection of 37 MBq of ^{125}I-35A7 at day 7 (Bip+ivd7-^{125}I-35A7-RIT) (n=7), or at day 11 (Bip+ivd11-^{125}I-35A7-RIT) (n=9). In order to assess the non-specific efficiency of ^{125}I-mAbs, another group was treated with Bip-RIT using 185 MBq of ^{125}I-PX mAb followed by i.v. injection of 37MBq of ^{125}I-PX mAb at day 7 (Bip+ivd7-^{125}I-PX-RIT).

Tumor growth was followed weekly by bioluminescence imaging. Mice were sacrificed when the bioluminescence signal reached a value of 4.5×10^7 photons/s corresponding to a total tumor weight of about 0.2—0.3g.

Bioluminescence and SPECT-CT imaging

In vivo bioluminescence imaging was performed following i.p. injection of luciferin (0.1 mg luciferin/g) as described in (*22*). Whole-body SPECT/CT images were acquired at various times following Bip-^{125}I-35A7-RIT (0 h, 1 h, 24 h and 72 h) with a two-headed multiplexing multi-pinhole NanoSPECT (Bioscan Inc., Washington DC).

Biodistribution experiments to mimic Bip-RIT and iv-RIT

On day 1, 48 athymic nude mice were i.p. grafted with 0.7×10^6 A-431 cells that had been suspended in 0.3 ml DMEM medium. Mice were divided in two groups to compare the biodistribution of ^{125}I-35A7 mAbs following Bip-RIT or iv-RIT. One group of mice was treated with Bip-^{125}I-35A7-RIT according to the previously described protocol but the injected solution contained 5.5 MBq (740MBq/mg) of ^{125}I-35A7 mAb completed with 243µg of unlabeled 35A7 mAb diluted in 5 mL. This group was called Bip-^{125}I-35A7-Biodis.

The second group was intravenously injected with a solution containing 185 KBq (740MBq/mg) of ^{125}I-35A7 mAb completed with 50µg of unlabeled 35A7 mAb diluted in 300 µL of saline solution (iv-^{125}I-35A7-Biodis).

Mice were sacrificed at 1, 24, 48, 72, 96, 144 and 168 h after treatment. At each time point, animals were anaesthetized, image acquisition by bioluminescence was performed and then they were euthanized, bled and dissected. Blood and other healthy organs were weighed. The size of tumor nodules was determined in order to calculate the tumor volume and thereby the tumor weight based on a density of 1.05g/cm^3 as described in Santoro *et al.* (*22*). The radioactivity uptake during the biodistribution experiments (i.e., UOR_{Biodis}) was then measured for tumor nodules and for all the organs using a gamma-well counter. The percentage of injected activity per gram of tissue (%IA/g), corrected for the radioactive decay, was calculated for iv-^{125}I-35A7-Biodis. For Bip-^{125}I-35A7-Biodis, results were expressed as percentage of the remaining activity per gram of tissue (%RA/g), immediately after the peritoneal wash (i.e. one hour after injection).

Tumor weight assessment during RIT experiments

Since accurate direct measurement of the weight of peritoneal tumors could not be performed in RIT experiments due to the high activities and also because it would require sacrificing the mice, it was calculated from the weekly bioluminescence imaging data. For this purpose, biodistribution experiments were used to determine the calibration curve between the bioluminescence signal of tumors and their size. Typically, prior to sacrifice, tumors were imaged by bioluminescence and the corresponding signal (photon/s) was correlated with the calculated tumor weight (g) determined by direct measurement of the size of tumor nodules, as described in (*22*). The calibration curve was similar to the one determined in our previous work (*22*).

Uptake of radioactivity per organ and tumor and dosimetry

The uptake of radioactivity per tissue (expressed in Becquerel) in RIT experiments (UOR_{RIT}) was extrapolated from the uptake per tissue (UOR_{Biodis}) measured during the biodistribution experiments. Since the activities used in RIT experiments were 33 times higher than those used in the biodistribution analysis (185 MBq *versus* 5.5 MBq) for the same amount of injected mAbs (250 µg), all the UOR_{Biodis} values were multiplied by 33 to mimic the therapeutic conditions. We considered that the weight of healthy tissues did not change all along the study period and that they did not differ between RIT and biodistribution experimental conditions. We confirmed that this assumption was true also for tumor nodules during the first week after injection. Therefore, the 33-fold correction was enough to determine the UOR_{RIT} from UOR_{Biodis}. The total cumulative decays per tissue, $\tilde{A}_{rs}$, were calculated by measuring the area under the UOR_{RIT} curves. Following the MIRD formalism (*25*), the resulting values were multiplied by the *S* factor for determining the irradiation doses as described in (*22*).

Statistical analysis

Kaplan-Meier survival estimates were calculated from the date of the xenograft until the date of the event of interest (i.e., a bioluminescence value of 4.5×10^7 photons/s) and compared with the Log-rank test. Statistical analysis was performed using the STATA 10.0 software.

RESULTS

Tumor growth

At day 4 after graft (just before starting the treatment), 5-6 nodules per mouse with a mean diameter of about 1.5-2 mm were detected by bioluminescence imaging. This corresponded to a mean tumor weight of $1.2\pm0.9 \times10^{-2}$ g. In the Bip-NaCl group, tumors grew exponentially and all mice were sacrificed before day 40 after graft (Fig. 1B). A similar growth rate was observed in mice treated by Bip+ivd7-^{125}I-PX-RIT (data not shown). The longest delay in tumor growth was observed in the Bip+ivd7-^{125}I-35A7-RIT group and intermediary tumor growth kinetics was reported for the Bip-^{125}I-35A7-RIT (Fig.1B), the Bip+ivd11-^{125}I-35A7-RIT and the ip+ipd7-^{125}I-35A7-RIT group (data not shown).

It is of note that the wash of the peritoneal cavity with NaCl slowed down tumor growth in the Bip-NaCl group compared to the ip-NaCl group (data not shown). This observation was further strengthened by the analysis of the survival data which was significantly lower after ip-NaCl ($p<0.001$, compare Fig. 3A with 3B).

Toxicity of Bip-RIT using ^{125}I-mAbs

The residual activity per mouse was about 14.2 ±7.3 MBq immediately after the wash with saline solution and dropped to 2.1 ±0.7 MBq at 120h after Bip-RIT (Fig. 1C). These results indicate that about 7.6% of the injected activity was effectively kept within the peritoneal cavity. No weight loss was observed after Bip-RIT (Suppl. Fig. 1). These results suggest that Bip-RIT is well tolerated by mice. However mild, transient hematological toxicity was reported in all treated mice in comparison to the control Bip-NaCl group (Fig. 2 and Suppl. Fig. 2). In the Bip-^{125}I-35A7-RIT group (Fig. 2), the nadir for white blood cells (WBC) was reached between day 7 and 10 (around -20%) after graft. It was mainly due to decrease in lymphocytes and monocytes levels (-40%) (Suppl. Fig. 2). Platelet lowest point occurred slightly later (days 10—15, -30%), while no modification in red blood cells was observed.

Most of the values returned to normal around day 39. In mice that received one intravenous injection of ^{125}I-mAbs at day 7 (Bip+ivd7-^{125}I-35A7-RIT, Bip+ivd7-^{125}I-PX-RIT), the decrease in WBC number was found to be more pronounced and prolonged (about -70% at day 22; Fig. 2). When the i.v. injection was done at day 11 (Bip+ivd11-^{125}I-35A7-RIT) after graft, the hematological toxicity was in the same range but more prolonged in time and values were not yet returned to baseline at day 39 (Fig. 2 and Suppl. Fig. 2). For day 52, the ratio could not be calculated since most of the mice in the Bip-NaCl group had to be sacrificed due to tumor growth.

The similar effects observed in the Bip+ivd7-^{125}I-35A7-RIT and Bip+ivd7-^{125}I-PX-RIT mice suggest that the hematological toxicity was mainly due to non-specific irradiation, including soft X-rays or the most energetic electrons emitted by ^{125}I. In addition, ip+ipd7-^{125}I-35A7-RIT (Fig. 2 and Suppl. Fig. 2) caused lower hematological toxicity than Bip+ivd7-^{125}I-35A7-RIT, despite the fact that higher activities were detected in ip+ipd7-^{125}I-35A7-RIT mice. Indeed, during the latter ip-RIT, 74 MBq (2×37 MBq) were effectively injected and available for diffusion towards blood compartment. By contrast, for Bip+iv-RIT among the 185 MBq used, only 14.2 MBq were remaining in mouse immediately after wash of the peritoneal cavity. This activity was completed by i.v. injection of 37 MBq, i.e. finally a total activity of 51.2 MBq was effectively remaining in mice. This result suggests that the high activity of 185 MBq maintained for one hour during Bip-RIT is mainly responsible for the hematological toxicity.

Bip-^{125}I-35A7-RIT improves survival of mice

Mice were sacrificed when the bioluminescence signal reached 4.5×10^7 photons/s corresponding to a mean tumor weight of about 0.2—0.3 g. The median survival (MS) was about 32 d in the Bip-NaCl group, but it significantly increased ($p<0.001$) to 46 d in the group treated with Bip-^{125}I-35A7-RIT (Fig. 3A). This value was significantly improved ($p<0.001$),

when Bip-RIT was combined with an i.v. injection at day 11 (Bip+ivd11-^{125}I-35A7-RIT) (MS = 66 d) or day 7 (Bip+ivd7-^{125}I-35A7-RIT) (MS = 73 d) (Fig. 3A). Moreover, one mouse in each of these two groups was cured at the end of the observation period of 100 d. Mice treated by Bip+ivd7-^{125}I-PX-RIT had an MS of 31 d rather similar to the control Bip-NaCl group ($p = 0.188$) (Fig. 3A), suggesting the absence of toxicity/efficiency of ^{125}I when unbound to cells. Finally, MS was 49 d in the ip+ipd7-^{125}I-35A7-RIT mice (Fig. 3B) and only 23 d in the ip+ipd7-NaCl-RIT control group ($p < 0.001$). Moreover one of the ip+ipd7-^{125}I-35A7-RIT mice was cured at the end of the period of interest.

SPECT-CT imaging after Bip-^{125}I-35A7-RIT

Whole body SPECT-CT imaging showed that after injection, radioactivity was homogeneously distributed in the peritoneal cavity (Fig. 4A). Following the wash of the peritoneal cavity the radioactivity concentrated at tumor nodules up to 3 d after injection (Fig. 4A), as indicated by the good fitting with the bioluminescence signals (Fig. 4B).

Bip-^{125}I-35A7-RIT improves tumor-to-healthy tissues uptake ratio

The biodistribution study confirmed the strong uptake of ^{125}I-35A7 mAbs by tumor nodules (Fig. 5A). The percentage of residual activity/g of tumor (%RA/g) immediately after the wash of the peritoneal cavity ranged between 72.1±30.2% at 1h and 20.5±4.8% at 168 h. These values were much higher than the peak value of 27.8±7.2% of injected activity/g of tumor (%IA/g) determined at 96h after a single i.v. injection of 37MBq (740MBq/mg), typical of intravenous ^{125}I-35A7-RIT (Fig. 5B). Moreover, the uptake of radioactivity by healthy organs was higher after i.v. injection than after Bip-^{125}I-35A7-RIT. For instance, in Bip-^{125}I-35A7-Biodis mice, the peak value in blood was observed at 48 h and was 12.2±3.2 %RA/g, while it was about 28.1±2.4%IA/g in the iv-^{125}I-35A7-Biodis group at 1 h after injection (Fig. 5B).

These results suggest that the Bip-^{125}I-35A7-RIT procedure improves tumor targeting and that healthy tissues are partially protected when compared to i.v. injection.

Cumulated uptake of radioactivity after Bip-^{125}I-35A7-RIT and dosimetry

From the biodistribution data, subsequently we expressed the uptake of radioactivity (UOR) of ^{125}I-35A7 mAb by healthy organs and tumor nodules as a function of time (Fig. 6A and 6B together with Suppl. Fig. 6A and 6B).

The cumulated uptake of radioactivity ($\tilde{A}_{rs}$) was then determined by calculating the area under the curves shown in Fig. 6A and 6B together with Suppl. Fig. 6A and 6B. According to the MIRD formalism, the mean absorbed irradiation dose per organ was calculated by multiplying $\tilde{A}_{rs}$ by the *S*-value corresponding to ^{125}I. The mean absorbed irradiation dose by tumors was 11.6 Gy after Bip-^{125}I-35A7-RIT and 16.7 Gy after iv-^{125}I-35A7-RIT. The irradiation dose delivered to healthy organs after Bip-^{125}I-35A7-RIT was much lower than after iv-^{125}I-35A7-RIT: for instance, blood received about 1.9 Gy after Bip-^{125}I-35A7-RIT and about 9.8 Gy after iv-^{125}I-35A7-RIT (Fig. 6C). The irradiation dose to the other organs did not exceed 1 Gy after Bip-^{125}I-35A7-RIT and 4.2 Gy after iv-^{125}I-35A7-RIT.

DISCUSSION

In the present study, we have investigated the feasibility, toxicity and efficacy of brief intraperitoneal RIT (Bip-RIT) using a ^{125}I-mAb directed against CEA. This protocol is based on the HIPEC methodology, although hyperthermia was not associated with Bip-RIT. Our results indicate that about 7% of the injected activity, corresponding to about 14.2 MBq, was retained in the peritoneal cavity after washing. Mild and transient blood toxicity was observed and was mainly due to non-specific irradiation (possibly soft X-rays and more energetic electrons emitted by ^{125}I) that occurred during the one-hour peritoneal incubation with high activities of ^{125}I-mAbs. However, we estimated that in patients, about 300 µGy would be delivered by such an external irradiation at the sacrum level (data not shown). Therefore, the hematological toxicity is expected to be much lower than in mice.

SPECT-CT imaging of mice at different time points after Bip-^{125}I-35A7-RIT and the biodistribution experiments indicate that radioactivity was concentrated in tumor nodules, whereas the irradiation dose to healthy organs by Bip-^{125}I-35A7-RIT was generally much lower than with iv-^{125}I-35A7-RIT and did not exceed 1Gy. In addition, although the irradiation dose delivered to the tumors was lower after Bip-^{125}I-35A7-RIT than after iv-^{125}I-35A7-RIT, the tumor-to-blood irradiation dose ratio was about 5 for Bip-^{125}I-35A7-RIT and 1.7 for iv-^{125}I-35A7-RIT, respectively. These results indicate that Bip-^{125}I-35A7-RIT protect healthy tissues while delivering significant irradiation doses to the tumors. This confirms the generally described advantage of i.p. over i.v. RIT for peritoneal disease in terms of concentration and tolerance (for review (*14*)). Therefore, although reducing the potential blood reservoir of ^{125}I-mAb in comparison to iv-RIT, the Bip-RIT procedure including the washing of the peritoneal cavity, eliminates undesirable radioactivity, and therefore it is less toxic.

The median survival of xenografted mice was significantly improved after Bip-^{125}I-35A7-RIT alone (46 d) in comparison to controls (32 d). However, the combination of Bip-^{125}I-35A7-RIT at day 4 and of iv-^{125}I-35A7-RIT at day 7 further increased survival time to 73 d. In our previous study (22), median survival was 59 d (*versus* 19 d for control) for mice treated with two i.v. injections of 37 MBq of ^{125}I-35A7 mAb. Assuming that the transient hematological toxicity we observed following Bip-^{125}I-35A7-RIT is effectively due to the initial one-hour incubation time with ^{125}I-mAbs in the peritoneal cavity, repeated i.v. injections of ^{125}I-mAbs could be planned after Bip-RIT or the combination of Bip-^{125}I-35A7-RIT and chemotherapy might be envisaged, without important increase of toxicity as we observed in the Bip+ivd7-^{125}I-35A7-RIT group. The median survival increased to 49 d also after two i.p. injections of anti-CEA mAbs (ip+ipd7-^{125}I-35A7-RIT) with low associated hematological toxicity. However, the effect on survival was less strong than the improvement obtained after Bip+ivd7-^{125}I-35A7-RIT (73 *versus* 49 d; while controls had a median survival of 32 and 23 d, respectively). Moreover, the uptake of radioactivity by healthy tissues during Bip-RIT was very low and probably much lower than during ip-RIT. In addition, the combination of Bip-RIT and iv-RIT takes advantage of the better peritoneal tumor uptake obtained through the i.p. route while the delayed i.v. injection may allow reaching pockets of cancer cells that were not targeted by Bip-RIT (*26*).

Completeness of resection and tumor load are the most important predictive factors of long-term survival after CRS-HIPEC. In the present study, we targeted tumor nodules of about $1.2\pm0.9 \times 10^{-2}$ g. It was demonstrated with beta emitters that RIT must be dedicated to small solid tumors (*27*). The size parameter is even more crucial when low energy electrons emitters are used as the path length of electrons emitted by ^{125}I ranges from nm to about 20µm while in peritoneal carcinomatosis tumor nodules have a diameter of several mm. Our results could be compared to the work by Aarts *et al.* in which the median survival of rats, which had CC-531

colon carcinoma tumor xenografts of few mm and were treated with a single i.p. injection of 74 MBq ^{177}Lu-labeled MG1 mAb, increased from 57 to 97 d when RIT was combined to CRS (*8, 9*). The low toxicity for healthy tissue of Auger electron emitters like ^{125}I is expected to be an advantage for the treatment of small peritoneal carcinomatosis, especially because it could allow combining radiation-synergistic chemotherapy, such as taxol (*28,29*), or drugs targeting the tumor microenvironment ((*30,31*) and for review (*32*)) with RIT. In addition, it makes also possible to repeat ^{125}I-mAbs injections. Precise mechanisms involved in the efficiency of ^{125}I-anti CEA mAb to delay tumor growth remain to be elucidated. Considering that most of the electron dose generated by ^{125}I decay is extremely localized, it means that most of the irradiation dose is delivered to the cell membrane when ^{125}I is vectorized by anti CEA mAb. Therefore, we can hypothesize that cell membrane is an important target of high-LET Auger electrons.

CONCLUSION

Our data confirm the efficiency of ^{125}I-anti CEA mAb in killing tumor cells. Bip-RIT is accompanied by a strong tumor-to-healthy tissues ratio that makes still possible to increase the injected activities while protecting healthy tissues. This is reinforced by the use of Auger electrons emitters like ^{125}I as they decrease non-specific irradiation. All these features might allow using repeated injections of radiolabeled antibodies or combining RIT with radiation-synergistic agents. Therefore, our results suggest that Bip-RIT with ^{125}I-labeled anti-CEA mAbs might be a complementary tool in the therapy of small solid tumors after CRS.

ACKNOWLEDGMENT

This work was supported by the Institut National du Cancer, grant R09080FF / RPT09005FFA. The authors would like to thank Imade Ait Arsa for animals care and involvement in experiments.

References

1. Glehen O, Mohamed F, Gilly FN. Peritoneal carcinomatosis from digestive tract cancer: new management by cytoreductive surgery and intraperitoneal chemohyperthermia. *Lancet Oncol.* 2004;5:219-228.

2. Glockzin G, Schlitt HJ, Piso P. Peritoneal carcinomatosis: patients selection, perioperative complications and quality of life related to cytoreductive surgery and hyperthermic intraperitoneal chemotherapy. *World J Surg Oncol.* 2009;7:5.

3. Sugarbaker PH. Comprehensive management of peritoneal surface malignancy using cytoreductive surgery and perioperative intraperitoneal chemotherapy: the Washington Cancer Institute approach. *Expert Opin Pharmacother.* 2009;10:1965-1977.

4. Sugarbaker PH, Cunliffe WJ, Belliveau J, de Bruijn EA, Graves T, Mullins RE, Schlag P. Rationale for integrating early postoperative intraperitoneal chemotherapy into the surgical treatment of gastrointestinal cancer. *Semin Oncol.* 1989;16:83-97.

5. Elias D, Gilly F, Boutitie F, Quenet F, Bereder J, Mansvelt B, Lorimier G, Dubè P, Glehen O. Peritoneal colorectal carcinomatosis treated with surgery and perioperative intraperitoneal chemotherapy: retrospective analysis of 523 patients from a multicentric French study. *J Clin Oncol*. 2010;28:63-68.

6. Elias D, Gilly F, Quenet F, Bereder JM, Sidéris L, Mansvelt B, Lorimier G, Glehen O. Pseudomyxoma peritonei: a French multicentric study of 301 patients treated with cytoreductive surgery and intraperitoneal chemotherapy. *Eur J Surg Oncol.* 2010;36:456-462.

7. Koppe MJ, Bleichrodt RP, Oyen WJG, Boerman OC. Radioimmunotherapy and colorectal cancer. *Br J Surg.* 2005;92:264-76.

8. Aarts F, Hendriks T, Boerman OC, Koppe MJ, Oyen WJG, Bleichrodt RP. A comparison between radioimmunotherapy and hyperthermic intraperitoneal chemotherapy for the treatment of peritoneal carcinomatosis of colonic origin in rats. *Ann Surg Oncol.* 2007;14:3274-82.

9. Aarts F, Bleichrodt R, de Man B, Lomme R, Boerman O, Hendriks T. The Effects of Adjuvant Experimental Radioimmunotherapy and Hyperthermic Intraperitoneal Chemotherapy on Intestinal and Abdominal Healing after Cytoreductive Surgery for Peritoneal Carcinomatosis in the Rat. *Ann Surg Oncol.* 2008; 15:3299-307.

10. Koppe MJ, Soede AC, Pels W, Oyen WJG, Goldenberg DM, Bleichrodt RP, Boerman OC. Experimental radioimmunotherapy of small peritoneal metastases of colorectal origin. *Int J Cancer*. 2003;106:965-972.

11. Kinuya S, Yokoyama K, Fukuoka M, Hiramatsu T, Mori H, Shiba K, Watanabe N, Shuke N, Michigishi T, Tonami N. Intraperitoneal radioimmunotherapy to treat the early phase of peritoneal dissemination of human colon cancer cells in a murine model. *Nucl Med Commun.* 2007;28:129-133.

12. Elgqvist J, Andersson H, Bäck T, Hultborn R, Jensen H, Karlsson B, Lindegren S, Palm S, Warnhammar E, Jacobsson L. Therapeutic efficacy and tumor dose estimations in radioimmunotherapy of intraperitoneally growing OVCAR-3 cells in nude mice with (211)At-labeled monoclonal antibody MX35. *J Nucl Med*. 2005;46:1907-1915.

13. Milenic DE, Brady ED, Garmestani K, Albert PS, Abdulla A, Brechbiel MW. Improved efficacy of alpha-particle-targeted radiation therapy: dual targeting of human epidermal growth factor receptor-2 and tumor-associated glycoprotein 72. *Cancer*. 2010;116:1059-1066.

14. Meredith RF, Buchsbaum DJ, Alvarez RD, LoBuglio AF. Brief overview of preclinical and clinical studies in the development of intraperitoneal radioimmunotherapy for ovarian cancer. *Clin Cancer Res*. 2007;13:5643s-5645s.

15. Alvarez RD, Huh WK, Khazaeli MB, Meredith RF, Partridge EE, Kilgore LC, Grizzle WE, Shen S, Austin JM, Barnes MN, Carey D, Schlom J, LoBuglio AF. A Phase I study of combined modality (90)Yttrium-CC49 intraperitoneal radioimmunotherapy for ovarian cancer. *Clin Cancer Res*. 2002;8:2806-2811.

16. Epenetos AA, Hird V, Lambert H, Mason P, Coulter C. Long term survival of patients with advanced ovarian cancer treated with intraperitoneal radioimmunotherapy. *Int J Gynecol Cancer*. 2000;10:44-46.

17. Meredith RF, Partridge EE, Alvarez RD, Khazaeli MB, Plott G, Russell CD, Wheeler RH, Liu T, Grizzle WE, Schlom J, LoBuglio AF. Intraperitoneal radioimmunotherapy of ovarian cancer with lutetium-177-CC49. *J Nucl Med*. 1996;37:1491-1496.

18. Hird V, Maraveyas A, Snook D, Dhokia B, Soutter WP, Meares C, Stewart JS, Mason P, Lambert HE, Epenetos AA. Adjuvant therapy of ovarian cancer with radioactive monoclonal antibody. *Br J Cancer*. 1993;68:403-406.

19. Nicholson S, Gooden CS, Hird V, Maraveyas A, Mason P, Lambert HE, Meares CF, Epenetos AA. Radioimmunotherapy after chemotherapy compared to chemotherapy alone in the treatment of advanced ovarian cancer: a matched analysis. *Oncol Rep*. 1998;5:223-226.

20. Verheijen RH, Massuger LF, Benigno BB, Epenetos AA, Lopes A, Soper JT, Markowska J, Vyzula R, Jobling T, Stamp G, Spiegel G, Thurston D, Falke T, Lambert J, Seiden MV. Phase III trial of intraperitoneal therapy with yttrium-90-labeled HMFG1 murine monoclonal antibody in patients with epithelial ovarian cancer after a surgically defined complete remission. *J Clin Oncol*. 2006;24:571-8.

21. Andersson H, Cederkrantz E, Bäck T, Divgi C, Elgqvist J, Himmelman J, Horvath G, Jacobsson L, Jensen H, Lindegren S, Palm S, Hultborn R. Intraperitoneal alpha-particle radioimmunotherapy of ovarian cancer patients: pharmacokinetics and dosimetry of (211)At-MX35 F(ab')2--a phase I study. *J Nucl Med*. 2009;50:1153-1160.

22. Santoro L, Boutaleb S, Garambois V, Bascoul-Mollevi C, Boudousq V, Kotzki P, Pèlegrin M, Navarro-Teulon I, Pèlegrin A, Pouget JP. Noninternalizing monoclonal antibodies are suitable candidates for 125I radioimmunotherapy of small-volume

peritoneal carcinomatosis. *J Nucl Med*. 2009;50:2033-2041.

23. Pouget JP, Santoro L, Raymond L, Chouin N, BardiÞs M, Bascoul-Mollevi C, Huguet H, Azria D, Kotzki P, Pelegrin M, Pelegrin A. Cell membrane is a more sensitive target than cytoplasm to dense ionization produced by Auger electrons. *Rad Res*. 2008;170:192-200.

24. Kohler G, Howe S, Milstein C. Fusion between immunoglobulin-secreting and nonsecreting myeloma cell lines. *Eur J Immunol*. 1976;61435:292-295.

25. Loevinger R, Budinger T, Watson E. MIRD Primer for absorbed dose calculations revised edition. New York: Society of Nuclear Medicine; 1991.

26. Goldenberg DM. Adjuvant and combined radioimmunotherapy: problems and prospects on the road to Minerva. *J Nucl Med* 2006;47:1746-1748.

27. Ychou M, Azria D, Faurous P, Quenet F, Saint-Aubert B, Rouanet P, PÞlegrin M, Guerreau D, Saccavini J, Mach J, Artus J, Pelegrin A. Adjuvant radioimmunotherapy trial with iodine-131-labeled anti-CEA monoclonal antibody F6 F(ab')2 after resection of liver metastases from colorectal cancer. *Clin Cancer Res*.2008; 14:3487-93.

28. DeNardo SJ, Kukis DL, Kroger LA, O'Donnell RT, Lamborn KR, Miers LA, DeNardo DG, Meares CF, DeNardo GL. Synergy of Taxol and radioimmunotherapy with yttrium-90-labeled chimeric L6 antibody: efficacy and toxicity in breast cancer xenografts. *Proc Natl Acad Sci U.S.A.* 1997;94:4000-4004.

29. Supiot S, Gouard S, Charrier J, Apostolidis C, Chatal J, Barbet J, Davodeau F, Cherel M. Mechanisms of cell sensitization to alpha radioimmunotherapy by doxorubicin or paclitaxel in multiple myeloma cell lines. *Clin Cancer Res*. 2005;11:7047s-7052s.

30. Burke PA, DeNardo SJ, Miers LA, Lamborn KR, Matzku S, DeNardo GL. Cilengitide targeting of alpha(v)beta(3) integrin receptor synergizes with radioimmunotherapy to increase efficacy and apoptosis in breast cancer xenografts. *Cancer Res.* 2002;62:4263-4272.

31. Pedley RB, El-Emir E, Flynn AA, Boxer GM, Dearling J, Raleigh JA, Hill SA, Stuart S, Motha R, Begent RHJ. Synergy between vascular targeting agents and antibody-directed therapy. *Int J Radiat Oncol Biol Phys*. 2002;54:1524-1531.

32. Chatal J, Davodeau F, Cherel M, Barbet J. Different ways to improve the clinical effectiveness of radioimmunotherapy in solid tumors. *J Cancer Res Ther*. 2009;5:S36-40.

Figure legends

Figure 1. A) Bip-RIT perfusing system. B) Tumor growth. The mean tumor weight per mouse was determined from the bioluminescence data obtained during the RIT experiments and using the calibration curve shown in Santoro *et al.* (*22*). C) Residual activity per mouse. Remaining activity in each mouse after washing of the peritoneal cavity (1h after injection) was determined by the biodistribution study. Values are the mean activity ± SD.

Figure 2. Hematological toxicity. White blood cells number was monitored at various times (0—39d) after Bip-^{125}I-35A7-RIT, Bip+ivd7-^{125}I-35A7-RIT, Bip+ivd11-^{125}I-35A7-RIT, Bip+ivd7-^{125}I-PX-RIT and Ip+ipd7-^{125}I-35A7-RIT and were expressed as a ratio of the number in treated and control mice.

Figure 3. Survival of treated mice. Athymic mice bearing intraperitoneal A-431 tumor cell xenografts were treated with ^{125}I-mAbs. Survival curves of A) Bip-NaCl, Bip-^{125}I-35A7-RIT, Bip+ivd7-^{125}I-35A7-RIT, Bip+ivd11-^{125}I-35A7-RIT, Bip+ivd7-^{125}I-PX-RIT treated mice; and B) ip-NaCl and ip+ipd7-^{125}I-35A7-RIT treated mice. Survival rates were estimated using the Kaplan-Meier method. Mice were sacrificed when the bioluminescence signal reached 4.5×10^7 photons /second. Censored mice are indicated on the graph by vertical bars.

Figure 4. Bioluminescence and SPECT-CT imaging. A) Bioluminescence imaging was carried out 4 d after graft, just before RIT. SPECT-CT imaging of a mouse treated by Bip-^{125}I-35A7-RIT (185MBq) at day 4 after graft: B) immediately after injection (0h) and at 1h, 24h or 72h after washing of the peritoneal cavity with saline solution.

Figure 5. Biodistribution analysis. Athymic nude mice bearing intraperitoneal A-431 tumor cell xenografts were treated by A) Bip-^{125}I-35A7-RIT. The percentage of residual activity per gram of tissue (%RA/g tissue) was determined in healthy organs and tumors immediately after washing of the peritoneal cavity. B) iv-^{125}I-35A7-RIT. The percentage of injected activity per gram of tissue (%IA/g tissue) was determined in healthy organs and tumors. Four mice were analyzed at each time point.

Figure 6. Uptake of radioactivity. Uptake of radioactivity per tissue (Bq) after A) Bip-^{125}I-35A7-RIT or B) iv-^{125}I-35A7-RIT, was determined using the values obtained during the biodistribution experiments (see Figure 5). For clarity, only the most representative results are shown and uptake values out of scale (0—1.5×10^{6} Bq) are shown in Suppl. Fig.6A and 6B. C) Mean absorbed irradiation dose for Bip-^{125}I-35A7-RIT and iv-^{125}I-35A7-RIT. From uptake of radioactivity curves, the total cumulative decay per tissue, $\tilde{A}_{rs}$, was calculated by calculating the area under each curve. $\tilde{A}_{rs}$ was then multiplied by 19.483 keV, which corresponds to the mean energy delivered at each ^{125}I decay.

A

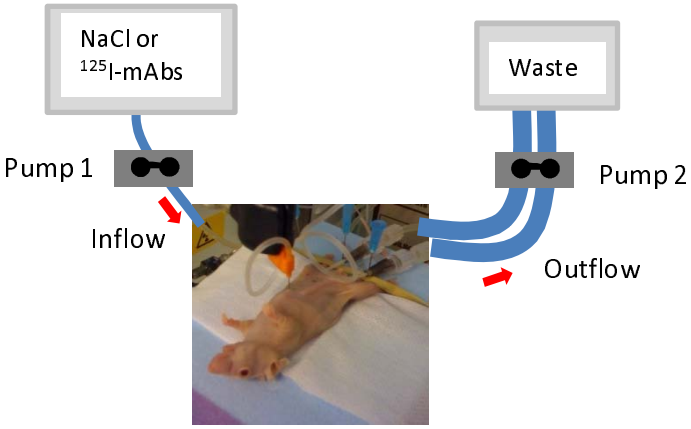
NaCl or
125I-mAbs
Waste
Pump 1
Pump 2
Inflow
Outflow

B

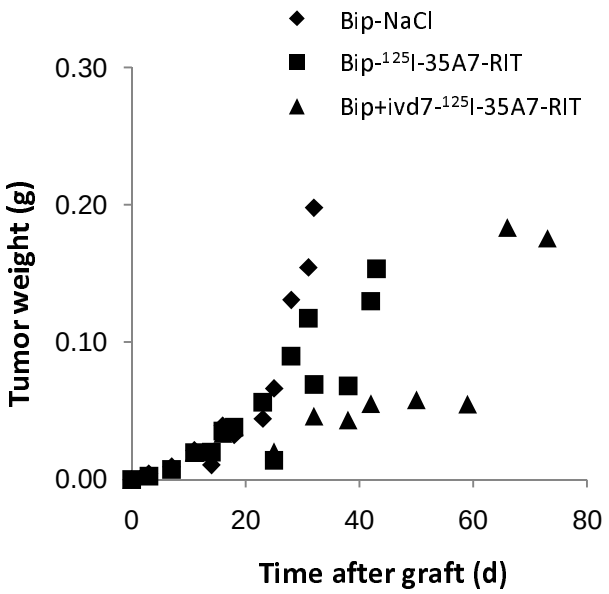
Bip-NaCl
Bip-125I-35A7-RIT
Bip+ivd7-125I-35A7-RIT
Tumor weight (g)
0.30
0.20
0.10
0.00
0
20
40
60
80
Time after graft (d)

C

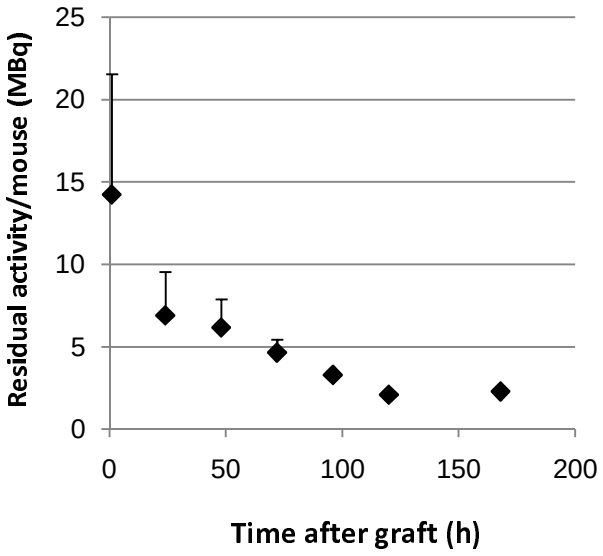
Residual activity/mouse (MBq)
25
20
15
10
5
0
0
50
100
150
200
Time after graft (h)

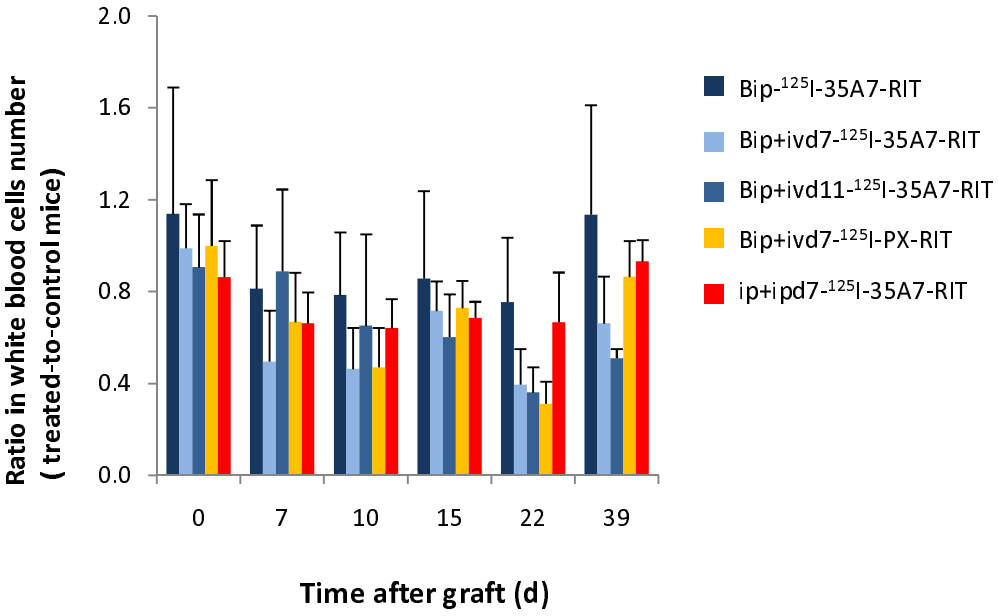
2.0
1.6
1.2
0.8
0.4
0.0
Ratio in white blood cells number
(treated-to-control mice)
0
7
10
15
22
39
Time after graft (d)
Bip-125I-35A7-RIT
Bip+ivd7-125I-35A7-RIT
Bip+ivd11-125I-35A7-RIT
Bip+ivd7-125I-PX-RIT
ip+ipd7-125I-35A7-RIT

A

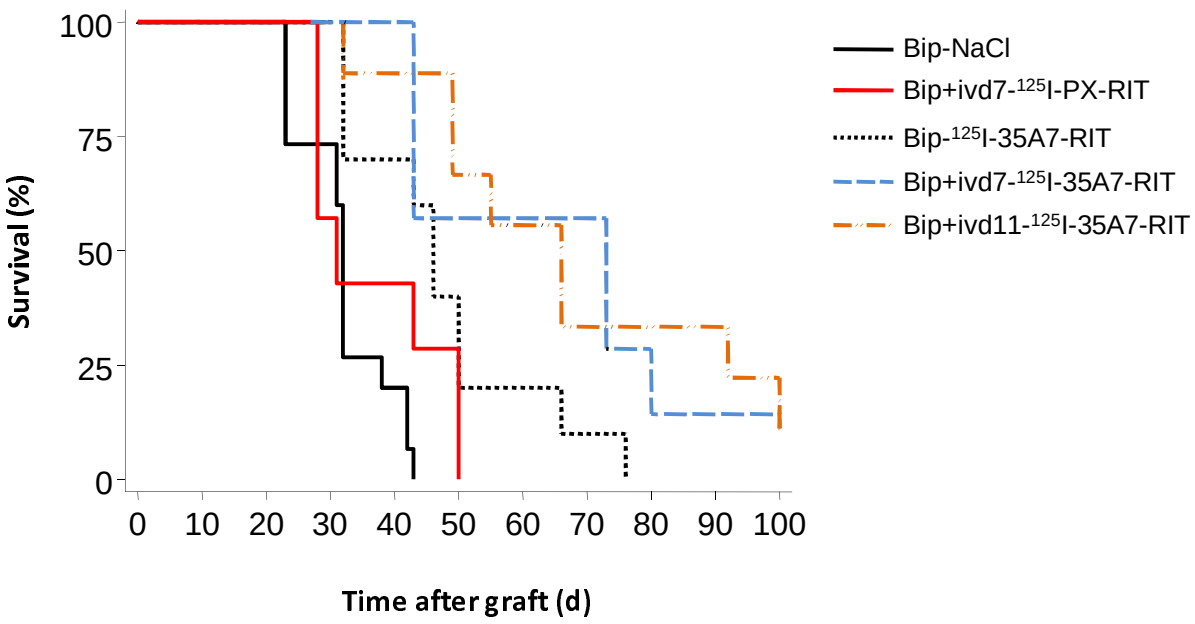
100
75
50
25
0
Survival (%)
0 10 20 30 40 50 60 70 80 90 100
Time after graft (d)
Bip-NaCl
Bip+ivd7-125I-PX-RIT
Bip-125I-35A7-RIT
Bip+ivd7-125I-35A7-RIT
Bip+ivd11-125I-35A7-RIT

B

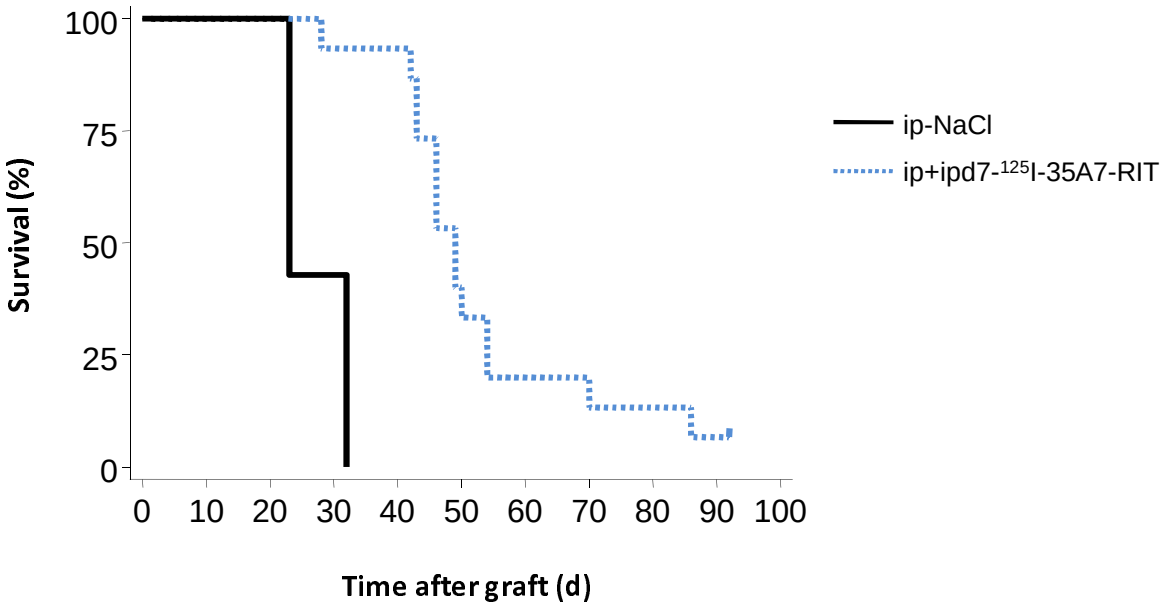
100
75
50
25
0
Survival (%)
0 10 20 30 40 50 60 70 80 90 100
Time after graft (d)
ip-NaCl
ip+ipd7-125I-35A7-RIT

A

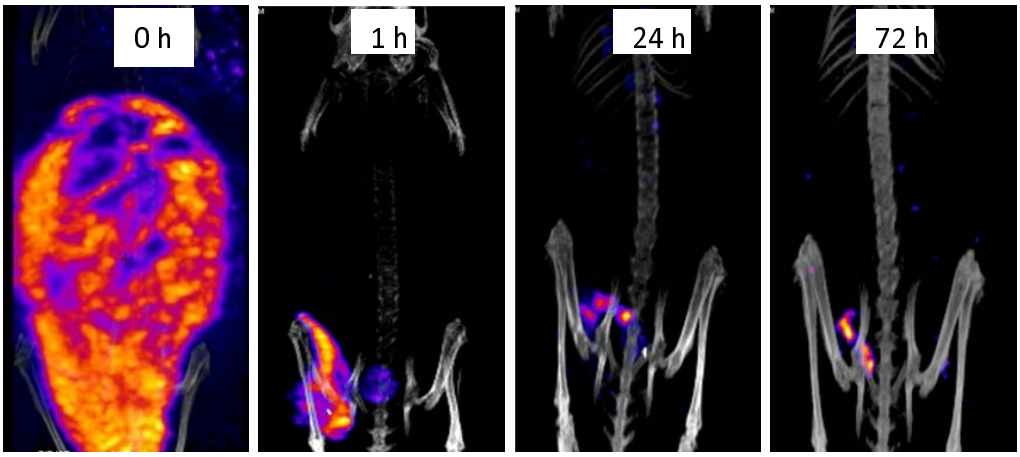

B

A

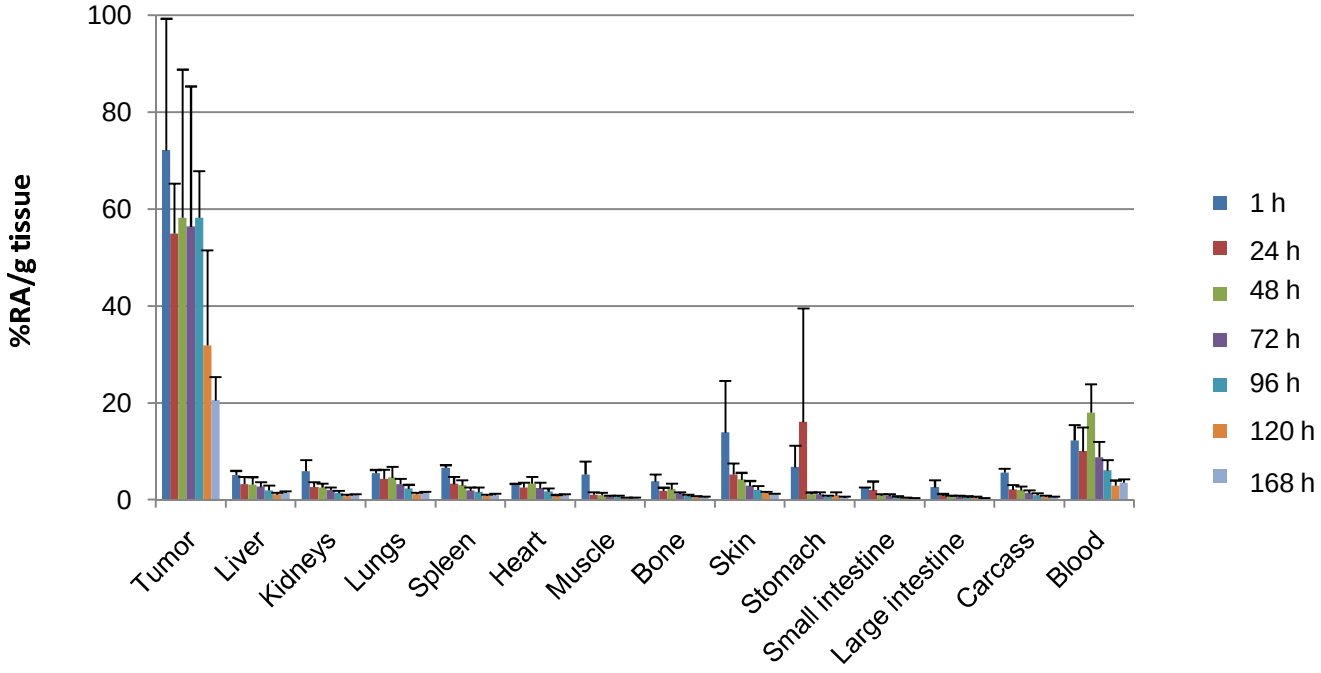
%RA/g tissue
100
80
60
40
20
0
Tumor
Liver
Kidneys
Lungs
Spleen
Heart
Muscle
Bone
Skin
Stomach
Small intestine
Large intestine
Carcass
Blood
1 h
24 h
48 h
72 h
96 h
120 h
168 h

B

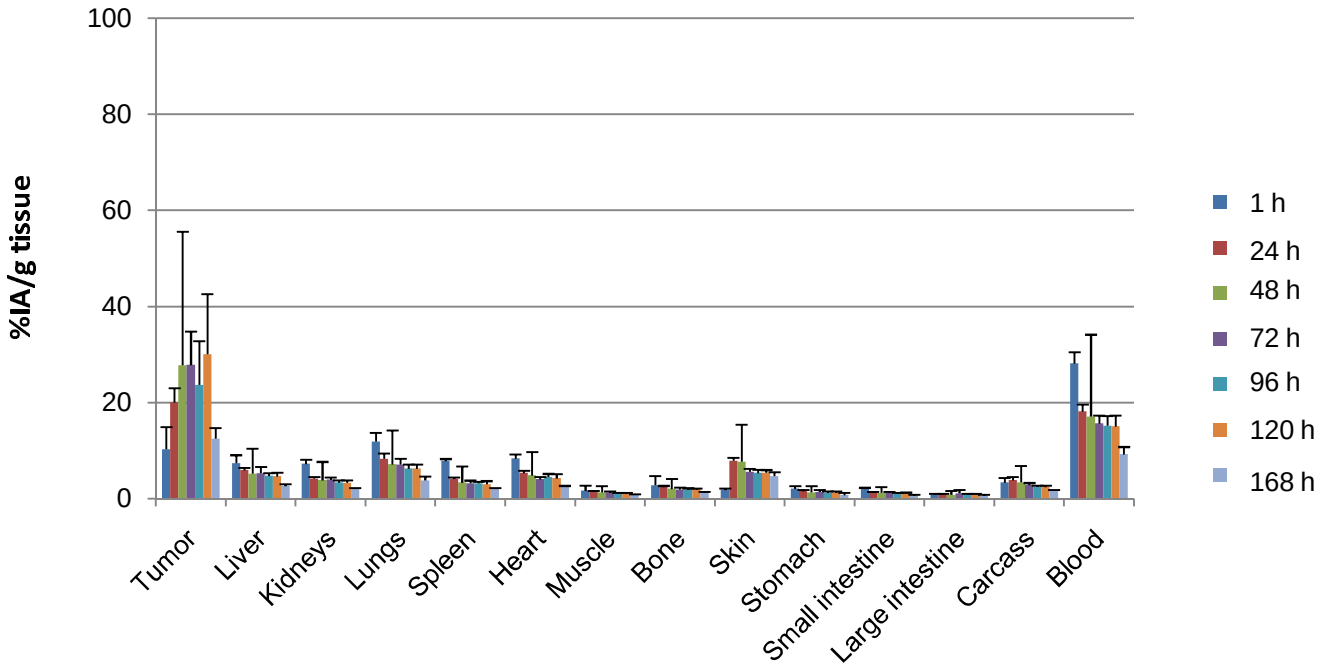
%IA/g tissue
100
80
60
40
20
0
Tumor
Liver
Kidneys
Lungs
Spleen
Heart
Muscle
Bone
Skin
Stomach
Small intestine
Large intestine
Carcass
Blood
1 h
24 h
48 h
72 h
96 h
120 h
168 h

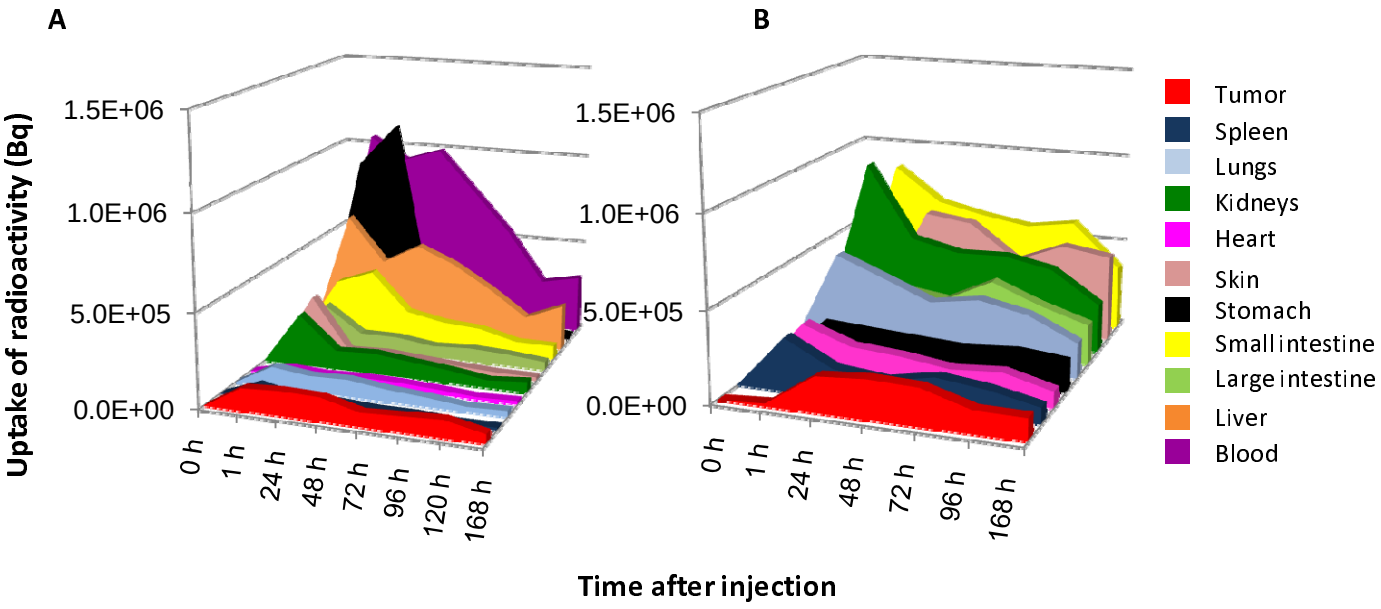
A
B
Uptake of radioactivity (Bq)
1.5E+06
1.0E+06
5.0E+05
0.0E+00
0 h
1 h
24 h
48 h
72 h
96 h
120 h
168 h
Time after injection
Tumor
Spleen
Lungs
Kidneys
Heart
Skin
Stomach
Small intestine
Large intestine
Liver
Blood

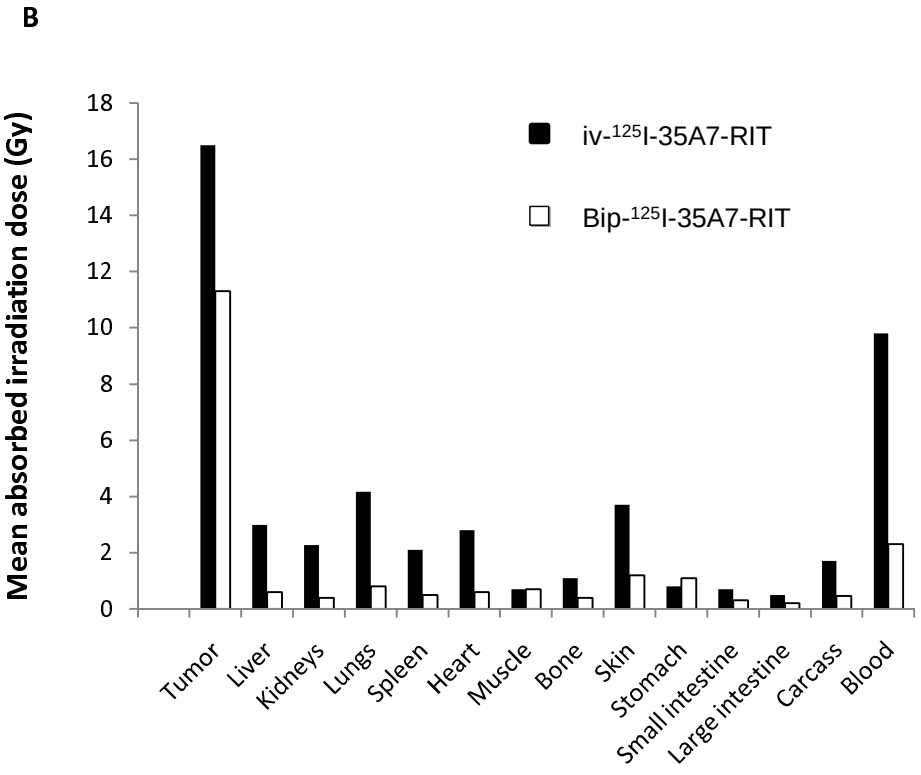
B
Mean absorbed irradiation dose (Gy)
18
16
14
12
10
8
6
4
2
0
iv-125I-35A7-RIT
Bip-125I-35A7-RIT
Tumor
Liver
Kidneys
Lungs
Spleen
Heart
Muscle
Bone
Skin
Stomach
Small intestine
Large intestine
Carcass
Blood